



OPEN

## Adherent cell remodeling on micropatterns is modulated by Piezo1 channels

Deekshitha Jetta<sup>1,4</sup>, Mohammad Reza Bahrani Fard<sup>1,4</sup>, Frederick Sachs<sup>2</sup>, Katie Munechika<sup>3</sup> & Susan Z. Hua<sup>1,2</sup>✉

Adherent cells utilize local environmental cues to make decisions on their growth and movement. We have previously shown that HEK293 cells grown on the fibronectin stripe patterns were elongated. Here we show that Piezo1 function is involved in cell spreading. Piezo1 expressing HEK cells plated on fibronectin stripes elongated, while a knockout of Piezo1 eliminated elongation. Inhibiting Piezo1 conductance using GsMTx4 or Gd<sup>3+</sup> blocked cell spreading, but the cells grew thin tail-like extensions along the patterns. Images of GFP-tagged Piezo1 showed plaques of Piezo1 moving to the extrusion edges, co-localized with focal adhesions. Surprisingly, in non-spreading cells Piezo1 was located primarily on the nuclear envelope. Inhibiting the Rho-ROCK pathway also reversibly inhibited cell extension indicating that myosin contractility is involved. The growth of thin extrusion tails did not occur in Piezo1 knockout cells suggesting that Piezo1 may have functions besides acting as a cation channel.

Cells detect and respond to mechanical cues with changes in shape, morphology, proliferation, and motility. This process is commonly thought to be mediated via adhesion proteins such as integrins at the adhesion complex<sup>1–3</sup>. However, Piezo (1 & 2) ion channels are sensitive to mechanical stress, suggesting that they may serve as a force coupling mechanism at cell adhesions. Piezo1 proteins are the subunits of trimeric non-selective mechanosensitive cation channels<sup>4–7</sup>. Piezo1 is expressed in many cell types where mechanical forces are thought to play a regulatory role<sup>5,8</sup>. For instance, Piezo1 in endothelial cells can detect shear stress in blood flow enabling alignment along the shear direction<sup>9,10</sup>. Piezo1 is able to transmit information about fluid shear stress to cell nuclei and modulate nuclear size and reorganization<sup>11</sup>. Piezo1 channels detect epithelial layer stretching and overcrowding, and can promote division of low density cells<sup>12</sup> or extrusion of crowded cells<sup>13</sup>. Piezo1 utilizes local environmental mechanical cues to regulate stem cell differentiation<sup>14</sup>. They also respond to osmotic pressure to regulate red cell volume via a Ca<sup>2+</sup>-dependent K<sup>+</sup> coupling<sup>15</sup>.

Piezo1 protein, originally called Fam38A, was first identified at locations side-by-side with integrins, that suggested Piezo1 and integrins may collaborate to regulate cell adhesion<sup>16</sup>. Via Piezo1, substrate stiffness alters the proportion of neurons to astrocytes during neural stem cell differentiation<sup>17</sup>. Similarly, in *Xenopus laevis*, substrate stiffness regulates the growth rate and direction of retinal ganglion cells (RGC)<sup>18</sup>. Activation of Piezo1 increased axon growth, in vitro and in vivo. On the other hand, a recent study discovered that age-related substrate stiffening caused oligodendrocyte progenitor cells to slow tissue regeneration<sup>19</sup>, and inhibiting Piezo1 recovered the functional activity of aged cells<sup>19</sup>.

The micropatterning of adhesive molecules has been widely used to provide mechanical inputs via spatial confinement. Cells grown on narrow stripe patterns stretch themselves along the axis<sup>20,21</sup>. Cells grown on T-shape patterns develop triangular shapes<sup>20,21</sup>. Using FRET based force probes, we previously reported that confinement by patterning the substrates caused a redistribution of tension within actinin during cell spreading<sup>20</sup>. Cells move faster on narrow patterns than broader substrates<sup>22,23</sup>. A recent study using Chinese hamster ovary (CHO) cells showed that a Piezo1 mediated Ca<sup>2+</sup> influx promoted migration of cells that are constrained on the pattern<sup>24</sup>.

Here we investigated the role of Piezo1 on cell shape and motility on narrow fibronectin stripes. We show that Piezo1 channels are essential for cell spreading on micro-patterns and knockout of Piezo1 eliminates cell expansion. However, inhibiting Piezo1 conductance with drugs leaves the cells with extended thin tail-like features, suggesting the Piezo1 may have additional roles other than mediating Ca<sup>2+</sup> signaling. Using a cloned Piezo1

<sup>1</sup>Department of Mechanical and Aerospace Engineering, University at Buffalo, Buffalo, NY 14260, USA. <sup>2</sup>Department of Physiology and Biophysics, University at Buffalo, Buffalo, NY 14260, USA. <sup>3</sup>Department of Biomedical Engineering, University at Buffalo, Buffalo, NY 14260, USA. <sup>4</sup>These authors contributed equally: Deekshitha Jetta and Mohammad Reza Bahrani Fard. ✉email: zhua@buffalo.edu

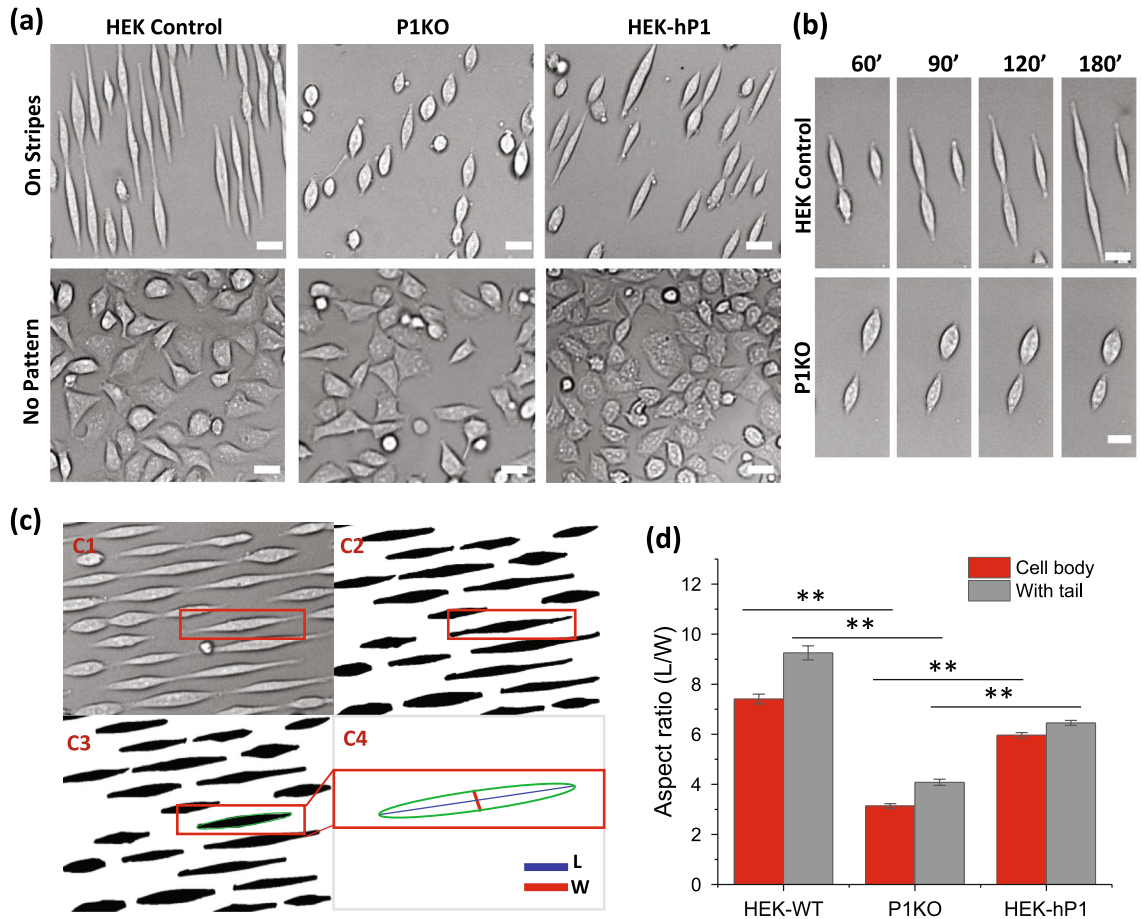


**Figure 1.** Role of Piezo1 on cell response to micropatterns. **(a)** Images of control, Piezo1 knockout (P1KO), and human Piezo1 expressing (hP1) HEK293T cells following fibronectin microstrips (upper panel), and controls for each cell types without patterning (lower panel). It shows that Piezo1 is required for cells' response to micropatterns. All images were taken 2.5 h after cell seeding. **(b)** Time sequence of cell expansion on stripes of control (upper panel) and P1KO cells (lower panel), showing P1KO cells lost the ability to elongate on the stripes. **(c)** Image processing steps. **(c1,c2)** show brightfield images were transformed to a binary image in MATLAB and cells were identified using “adaptive threshold”. **(c3)** After an erosion and a dilation operation, the cell bodies were restored while the tail-like features were removed. **(c4)** Individual cells were fitted with ellipses and the ratio of major and minor axes of the ellipses was defined as the aspect ratio. **(d)** Statistical analysis of the aspect ratio of cell body (red) and cell body with tails (gray) for each cell type ( $n = 120$  from more than 6 experiments for each cell type,  $**p < 0.001$ ). Scale bars represent 20  $\mu\text{m}$ .

expressing HEK cell line, HEK-hP1, we show that Piezo1 proteins co-locate with focal adhesion complexes at the tips of spreading cells and this process involves myosin-II contractility via a Rho-ROCK pathway.

## Results

**Piezo1 is required for cell spreading on the micropatterns.** We previously reported that HEK cells show elongation along micropatterned fibronectin stripes<sup>20</sup>. To access the role of Piezo1 in cell shaping, we tested a Piezo1 knockout in HEK293 cells (P1KO) on the same fibronectin stripes (6  $\mu\text{m}$  wide, 10  $\mu\text{m}$  spacing), and compared the results with control cells and with HEK293T cells stably transfected with EGFP-tagged human Piezo1 (HEK-hP1)<sup>25</sup>. All three cell types attached to the fibronectin surfaces within  $\sim 15$  min after seeding, and reached a maximum extension in  $\sim 2.5$  h.

Compared with control and HEK-hP1 cells (Fig. 1a, SM movie 1), P1KO cells were not able to stretch to a large extent on the stripes within the experimental period, although they exhibited some ability to move axially (Fig. 1a, SM movies 2). The control cells showed the largest elongation on the stripes (Fig. 1a). HEK-hP1 cells also spread well (Fig. 1a, SM movie 3). The time course of typical P1KO cells linear expansion compared with control cells showed that the control cells expanded for  $\sim$  threefold longer than P1KO cells (Fig. 1b). On uniformly coated fibronectin cover slips, the three cell types showed negligible differences in shape (Fig. 1a, lower panel). This suggests that assays based upon open substrates may conceal critical differences in cell physiology.

To quantify the effect of substrate confinement on cell shape, we developed an image processing algorithm including the following steps (see method section for details). Briefly, brightfield images were transformed to binary images and cells were identified using “adaptive threshold”. The output binary images included full cell length (cell body with tails, Fig. 1,c1,2). Some cells showed tail-like thin features at the tips under drug treatments

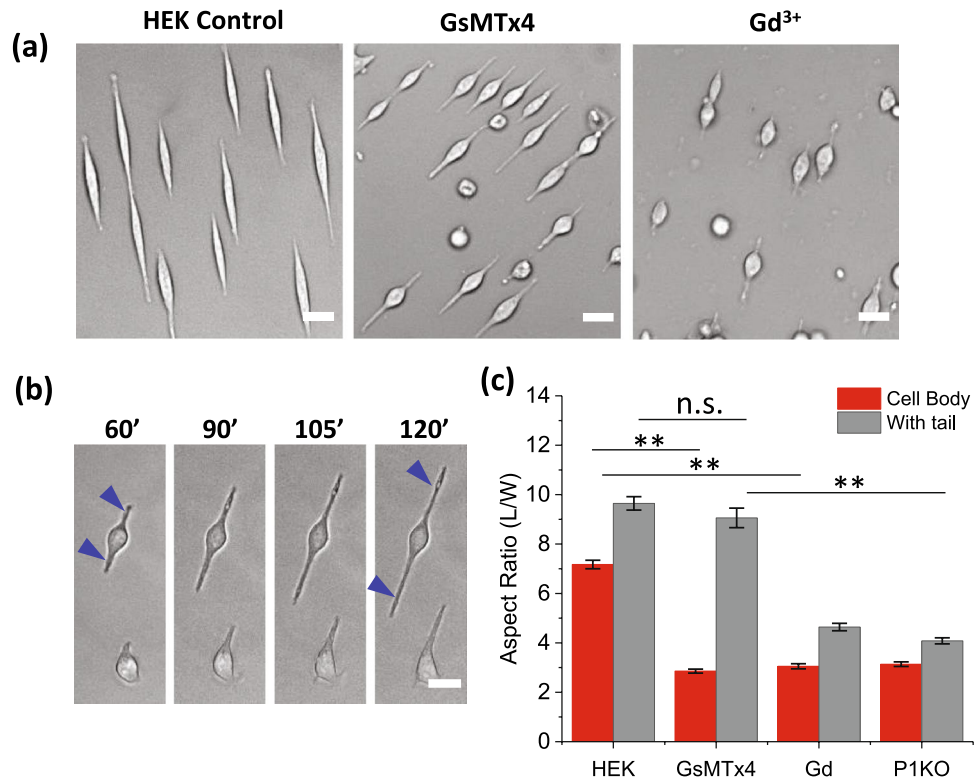


**Figure 2.** Effect of Piezo1 inhibitors on cell spreading on patterns. **(a)** HEK cells grown on fibronectin stripes in control solution, GsMTx4 (20  $\mu$ M), and Gd<sup>3+</sup> (60  $\mu$ M) for 2.5 h, showing inhibiting Piezo1 channels eliminated cell expansion. Drugs were added 15 min after seeding. **(b)** Cell reshaping on stripes in the presence of GsMTx4, showing thin tail-like spikes (indicated by blue arrows) while the cell body remained unchanged. **(c)** Mean aspect ratios (with and without counting the tail length) of cells in media and in the presence of inhibitors (n = 120 for each condition and from multiple experiments, \*\* $p$  < 0.001). Scale bars represent 20  $\mu$ m.

(later sections). An erosion was applied to the images which removed the fine structures in the image; this was followed by a dilation with the same parameter as the erosion to restore the cell body shapes while the tails were removed (cell body, Fig. 1, c3). The major and minor axes of the best fitted ellipse were calculated for cell body and for cell body with tails, respectively. The ratio of the major axis to the minor axis (L/W) of an ellipse was defined as the aspect ratio of a cell (Fig. 1, c4).

The aspect ratios of control and HEK-hP1 cells were significantly larger than P1KO cells (Fig. 1d, n = 120, \*\* $p$  < 0.001). Although HEK-hP1 cells have slightly lower aspect ratio than control cells, these cells spread more evenly throughout the elongation compared with control cells that showed narrower tips (Fig. 1a). In addition, HEK-hP1 cells were more active than the control cells. For a given frame, some cells were in elongation and some were in retraction (SM Fig. 1).

**Inhibiting Piezo1 channels inhibited cell spreading.** Piezo1 proteins function as mechanosensitive cation channels (MSCs) that open with membrane tension<sup>4,8,26</sup>. Piezo1 mediated Ca<sup>2+</sup> influx in HEK cells promotes migration<sup>25</sup>. To investigate the functional role of Piezo1 channels on cell elongating, we inhibited the channels with the known Piezo1 inhibitor, GsMTx4<sup>26</sup>. Cells did not stretch to a full extent in the presence of GsMTx4 (Fig. 2a). Some cells exhibited an interesting feature; a small cell body connected with long narrow tail-like features (Fig. 2b). While the body length (defined by abrupt change in thickness and width) remained constant, the tails elongated along the stripe (Fig. 2b). They do not expand laterally to cover the patterned surface. As controls, we inhibited mechanosensitive channels using the non-specific inhibitor Gd<sup>3+</sup>, and it too inhibited cell expansion but allowed the narrow tails (Fig. 2a). The tail-like feature was not observed in P1KO cells (Fig. 2c, n = 120, \*\* $p$  < 0.001). These results suggest that Piezo1 may have multiple roles in cell expansion. Cell body expansion requires *opening* of Piezo1 channels with cation currents, likely via a Ca<sup>2+</sup> influx. However, the growth of thin spikes only requires the *presence* of Piezo1, possibly through their interaction with integrins since they co-localize at cell protrusion edges (see below).

**Piezo1s translocate to the extrusion edges during cell elongating.** To investigate the distribution of Piezo1 during cell elongating, we followed GFP labeled Piezo1 in HEK-hP1 cells, and found that Piezo1 plaques continuously translocate from the middle of the cell to the cell extrusion edges during expansion (Fig. 3a, SM Movie 4). When cells reached a maximum length at ~ 2.5 h, the Piezo1 plaques accumulated at the extrusion

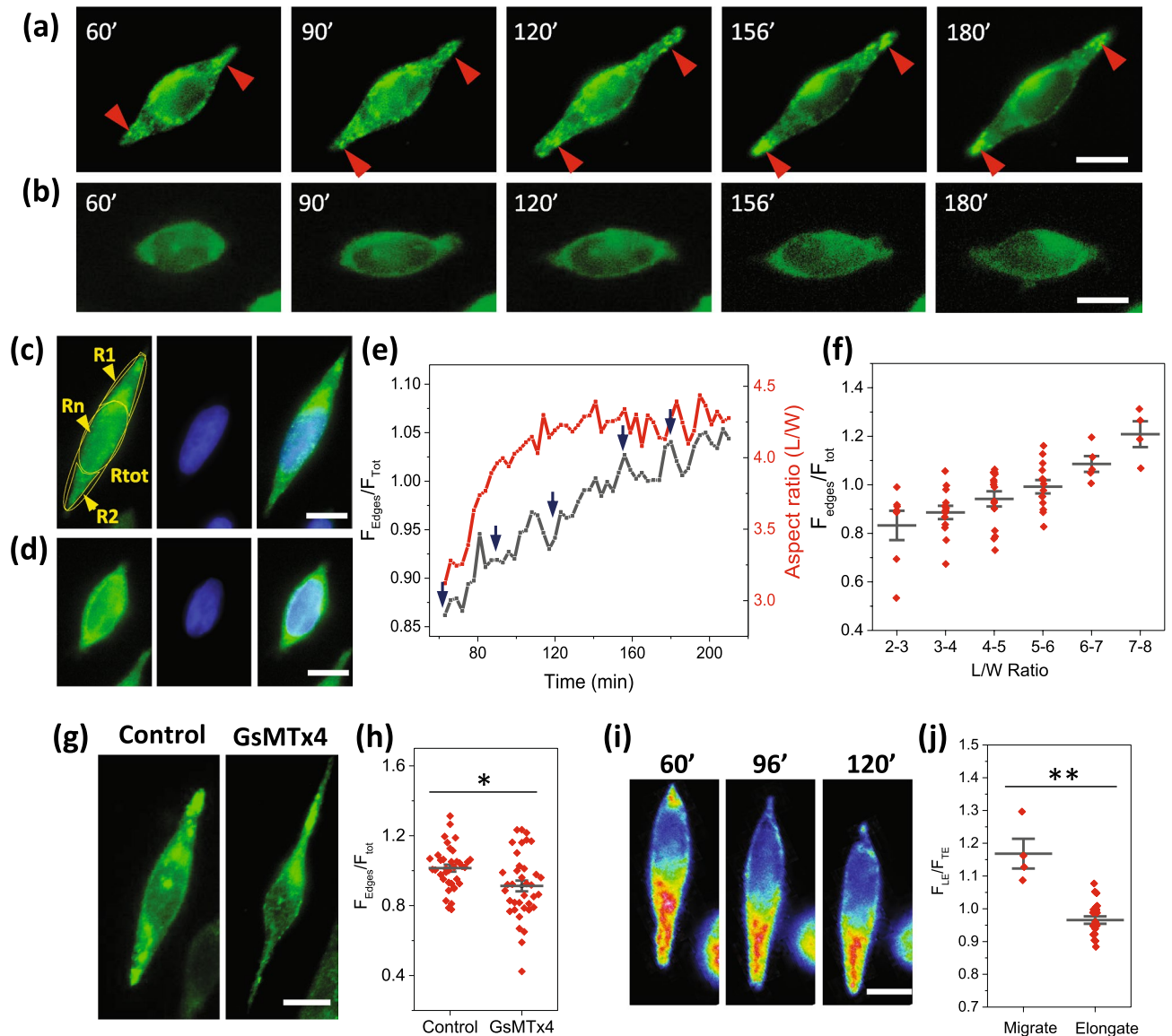


**Figure 3.** Redistribution of Piezo1 in HEK-hP1 cells on micropatterns. **(a)** Images of typical HEK-hP1 cell extending on the pattern from times indicated by blue arrows in **(e)**, showing Piezo1 plaques (indicated by red arrows) are present on the extrusion edges of an extending cell. **(b)** shows Piezo1 primarily distributed around the nuclear envelope in non-extending cells. The nucleus was stained using Hoechst 33342 dye for an extending **(c)** and a non-extending cell **(d)**. **(e)** Time course of average Piezo1 density over expansion edges (R1 and R2) normalized with whole cell (left axis) is compared with cell aspect ratio (right axis) of the cell in **(a)**, showing increased Piezo1 concentration is correlated with cell expansion. **(f)** Histogram of normalized Piezo1 density at the expansion edges of cells elongated to various aspect ratios, showing higher Piezo1 density corresponding to larger expansion ( $n=7, 14, 15, 14, 5, 4$ , sequentially). **(g)** Fluorescence images show that Piezo1 clusters remained in the tails in the presence of GsMTx4. **(h)** Relative Piezo1 density in the tails following GsMTx4 is slightly lower compared with control cells ( $n=37, p=0.007, *p<0.01$ ). **(i)** Time sequence of Piezo1 distribution in a migrating cell shows a significantly higher Piezo1 density at the leading edge. **(j)** Comparison of Piezo1 density in the leading edge compared to the trailing edge between migrating and stably elongated cells ( $n=25$  for elongating cells,  $n=4$  for migrating cell,  $**p<0.001$ ), from multiple experiments. Scale bars represent  $10\ \mu\text{m}$ .

edges (indicated by red arrows in Fig. 3a). In non-stretching cells, Piezo1 proteins were primarily located on the nuclear envelopes or in the middle of the cells (Fig. 3b). This is shown by staining the nucleus with Hoechst 33342 dye (Fig. 3c,d). Piezo1 density around nucleus (Fig. 3c, Rn), in expansions beyond the nucleus (Fig. 3c, R1 and R2), and the whole cell (Fig. 3c, Rtot) were measured, respectively, and the density in both expansions was averaged and normalized by the total density over the whole cell. The time course of the Piezo1 density at the edge and the corresponding body aspect ratio in Fig. 3a is shown in Fig. 3e. An increase in Piezo1 density in extrusion edges coincided with elongation. The mean Piezo1 density at extrusion edges for various cell aspect ratios is shown in Fig. 3f. The edge protein density was consistently higher in stretching than non-stretching cells. In cells treated with GsMTx4, Piezo1 clusters remained in the tails (Fig. 3g). The Piezo1 density in some

tails was comparable with controls, but it was much lower in other tails. This leads to a slightly lower mean density compared with control cells (Fig. 3h,  $n = 37$ ,  $p = 0.007$ ). This result suggests that Piezo1 is involved in cell elongation but not via its ion conduction properties. In control cells on a uniform glass surface, Piezo1 is mostly located in the cell body or scattered at the cell periphery but we observed no significant number of Piezo1 plaques. The aggregation of Piezo1 into plaques seems to be driven by the physiology required to extend the cells in a confined geometry.

Piezo1 density is significantly higher at the leading edge than the trailing edge of migrating cells (Fig. 3i, SM Movie 5). The distribution of Piezo1 in migrating cells compared with immobile but extending cells showed that Piezo1 locates toward the advancing edge of both cell types (Fig. 3j). Cell motility was decreased by GsMTx4 and  $Gd^{3+}$ , although Piezo1 still concentrated at the advancing cell edges (Fig. 3g). A recent study using Chinese hamster ovary (CHO) cells showed that a  $Ca^{2+}$  elevation occurred in migrating cells growing on narrow stripes<sup>24</sup>. This result is consistent with our earlier report that Piezo1 activity facilitated cell migration<sup>25</sup>.

**Piezo1 co-localized with FAs in extending cells.** To see whether the translocation of Piezo1 plaques correlates with the formation of focal adhesions (FAs) during cell expansion, we tested Piezo1 in HEK-hP1 cells co-transfected with mApple-tagged paxillin. Piezo1 plaques at the extrusion edges collocated with FAs in elongating cells but not in resting cells (Fig. 4a). The two labels overlapped in some cells, and appeared side by side in others (Fig. 4b). Although the presence of Piezo1 is necessary for elongation, we cannot tell whether there is an intermolecular reaction between Piezo1 and paxillin or other FA proteins. The FA and Piezo1 plaques only formed at cells extrusion edges in elongated cells. In control cells on glass, Piezo1 is primarily located in the middle of the cell and scattered along the cell periphery (Fig. 4c). We did not observe co-localized mature FAs with Piezo1 clusters at the cell edges (Fig. 4b, from  $n = 62$  patterned cells and  $n = 25$  control cells). Piezo1 can be recruited to FAs<sup>27</sup>, our results show that co-localization of Piezo1 and FAs does not occur when the cells are in the relaxed state.

**Rho-ROCK pathway is involved in cell spreading.** We previously reported that change in cell shape and expansion over patterned surfaces is a force sensitive process that requires functional actomyosin Rho-ROCK pathways<sup>20</sup>. We tested whether Rho-regulated myosin-II contraction force plays a role in translocation of Piezo1 proteins and the opening of Piezo1 channels. We inhibited Rho-ROCK pathways with the ROCK inhibitor Y27632, and it reversibly inhibited cell expansion (Fig. 5a). In the presence of inhibitor, the cell body shrank, but the tail-like feature remained. After washout, the cells regained full expansion (Fig. 5a). The effect of inhibitor was consistent in HEK-hP1 and control cells (Fig. 5b, also see SM Fig. 2). This suggests that Rho-II associated contractile forces affect Piezo1 channel functions required for cell full spreading. The density of Piezo1 in the cell edges was slightly lower under Y27632, despite cell shrinkage (Fig. 5c,d). The cells exhibited similar tail-like feature as they had under GsMTx4 (Fig. 3g). The translocation of Piezo1 to the extrusion edge of the cell was not reversible. This result is consistent with our previous report that Rho-II associated contractility could lead to changes in membrane tension that opens Piezo1 channels causing cell expansion.

## Discussion

Adherent cells respond to mechanical cues such as spatial confinement on patterned substrates. Our results show that knockout of Piezo1 inhibited cells' ability to respond to the pattern (Fig. 1), demonstrating that Piezo1 is involved in this process. Blocking Piezo1 channels with inhibitors, GsMTx4 and  $Gd^{3+}$ , inhibited the overall cell expansion measured by aspect ratio of cell body on the pattern, but cells grew a thin, long, tail-like feature. This result that inhibition of Piezo conductance is not the same as the knockout indicates that Piezo1 may have roles besides ion conductance on cell shape. The full spreading of cells requires Piezo1 mediated current. During cell expansion, Piezo1 clusters moved from the cell soma to the extrusion edges. Piezo1 plaques co-localized with the FA complexes at the extrusion edges elongating cells. The body expansion, but not the thin tails, was eliminated by the ROCK inhibitor, suggesting that both Piezo1 and Rho-ROCK signaling are functional in fully spreading cells.

Piezo1 is a mechanosensitive ion channel, reputed to regulate cell physiologies via  $Ca^{2+}$  signaling<sup>4,5</sup>. Wild-type HEK293T cells express endogenous Piezo1 channels<sup>7</sup>, that could be opened during cell expansion activating  $Ca^{2+}$ -dependent downstream pathways leading to cell remodeling. Inhibiting Piezo1 channel activity inhibited cell expansion, indicating the ion influx mediated by Piezo1 plays a role consistent with the observation that fluid shear stress caused a  $Ca^{2+}$  influx in HEK293T cells through Piezo1 channels<sup>25,28</sup>. However, inhibiting Piezo1 conductance only inhibited the full cell spreading; cells still grew the long thin spikes (Fig. 2). Since GsMTx4 or  $Gd^{3+}$  may not be specific for a particular MSC, some other MSCs such as TMEM63,  $K_{2P}$ , and TRPs could be involved<sup>29</sup>. Recent reports indicate that TMEM63A/B/C in transfected HEK cells can be activated by mechanical stimulation<sup>30</sup>. TRPV4 was also found to contribute to currents activated by stimuli applied at cell-substrate contacts<sup>31</sup>. GsMTx4 relaxes membrane tension by inserting into the membrane under stretching<sup>32</sup>, thus it could inhibit the activity of all mechanosensitive membrane proteins. The cell expansion was largely reduced in PIKO cells suggesting that Piezo1 channels play an essential role, possibly because Piezo1 channels have lower activation thresholds than other MSCs<sup>29</sup>. Piezo1 may have roles in cell elongating in addition to its functions on  $Ca^{2+}$  influx. Piezo1 protein, originally called Fam38A, was first identified at locations side-by-side with integrins, suggesting that Piezo1 and integrins collaborate to regulate adhesion<sup>16</sup>. As Coste et al<sup>5</sup> pointed out, disrupting integrin signaling does not affect Piezo1 current suggesting that activation of Piezo1 could lead to integrin activation, not the other way round<sup>5</sup>. Our results demonstrate that thin cell extrusion growth does not require the opening of the channels.

During cell spreading, Piezo1 clusters continuously translocate from soma to extrusion edges forming plaques at the cell tips (Fig. 3). The relative protein density at the spreading edges in stretching cells is higher than

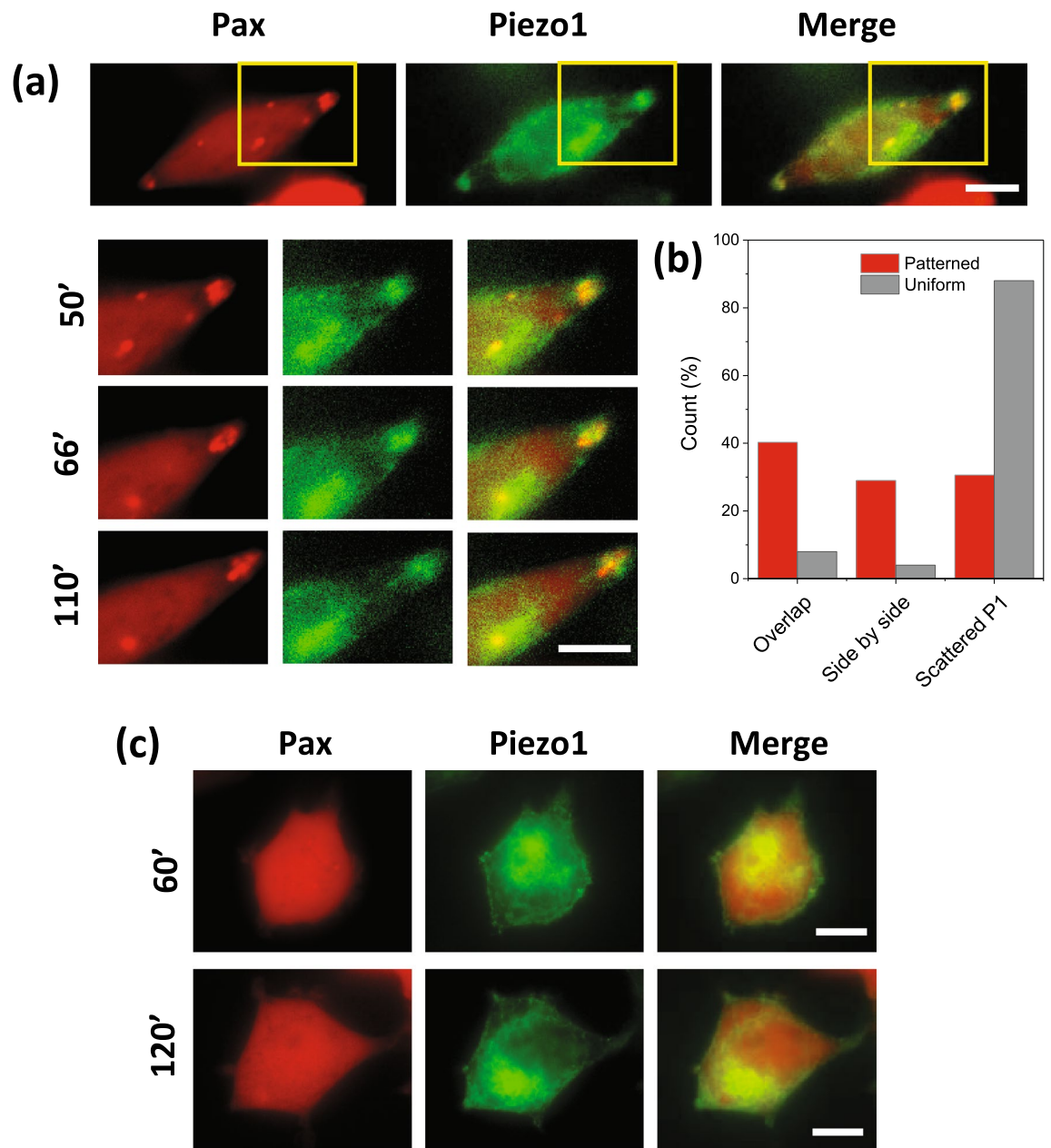


**Figure 4.** Piezo1 plaques correlate with FAs at the cell extrusion edges on the pattern. **(a)** Images of a typical HEK-hP1 cell (Piezo1, green) co-expressing mApple-paxillin (red); the zoomed view shows the co-localization between Piezo1 plaques and FAs at the extrusion edge at various times during cell elongation. **(b)** Statistical data shows that the two proteins collocated in most elongated cells, but side by side in some cells ( $n = 62$  for patterned cells,  $n = 25$  for control cells). **(c)** Images of paxillin and Piezo1 in a control cell (without pattern) show that there are no mature FAs present at the cell edges. Scale bars represent  $10 \mu\text{m}$ .

non-stretching cells. In migrating cells, the Piezo1 distribution is polarized and mainly located at the leading edge. The redistribution of Piezo1 proteins was only observed in the cells on narrow stripes that imposed a mean tension gradient on the cell. On uniform substrates, Piezo1 is mostly located in the middle of the cell. A previous study by the Rosenblatt group shows that Piezo1 overexpression occurred at the cell edges of sparse regions where the cell membrane was expanded<sup>12</sup>. The redistribution of Piezo1 proteins is sensitive to the stresses in cells such as cytoskeletal stress and correlated membrane tension.

It is widely recognized that cells use transmembrane integrins at focal adhesions to translate extracellular matrix (ECM) mechanical cues to the cytoskeleton to facilitate cell remodeling<sup>1-3</sup>. Our study shows that Piezo1 plaques co-localize with mature FAs at cell expansions. Although Piezo1 proteins exist in the thin tail-like features, no mature FAs were observed in those domains. Without the patterns, neither distinct Piezo1 plaques nor mature FAs were observed along the cell periphery (Fig. 4). A recent study has shown that Piezo1 is recruited

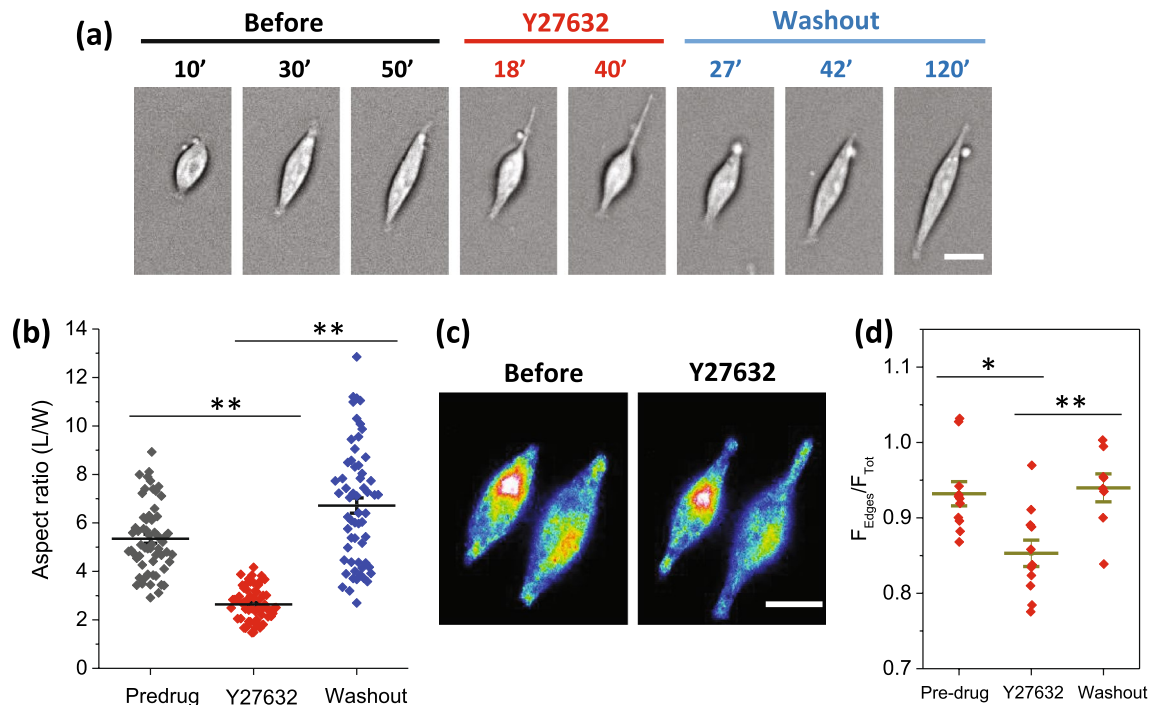


**Figure 5.** Effect of Rho-ROCK inhibitor on cell elongation. **(a)** Cell's response to Rho-ROCK inhibitor Y27632 followed by washout, showing Y27632 reversibly inhibited cell elongation. The times measured from the beginning of each process, seeding, drug application, and washout, respectively. Scale bar represents 10  $\mu$ m. **(b)** Mean aspect ratio for pre-drug treatment, 20 min after treatment, and 100 min after washout, shows that the drug effect is statistically significant ( $n = 60$  for each condition from 6 experiments,  $**p < 0.001$ ). **(c)** GFP images of a typical HEK-hP1 cell before and after application of Y27632, showing Piezo1 proteins remained at the cell edges although the cell body contracted under the drug. Scale bars represent 10  $\mu$ m. **(d)** Relative Piezo1 density in cell extensions in the presence of Y27632 is slightly lower compared with before and after washout ( $n = 11$  for pre-and under drug,  $n = 8$  for washout,  $*p < 0.01$ ,  $**p < 0.001$ ).

to FAs in normal cells but not in transformed cells including HEK<sup>27</sup>, that observation was done on a uniform substrate, consistent with our control cells.

Our results further show that cell expansion on the pattern can be reversibly inhibited with the Rho-ROCK inhibitor Y27632, although the tail-like features remained (Fig. 5). This suggests that Rho-ROCK activated Myosin-II contractile force affects Piezo1 mediated  $Ca^{2+}$  influx required for full cell expansion but not Piezo1 translocation. It is known that Myosin-II contractile force regulates the formation of focal adhesions and actin assembly through a  $Ca^{2+}$ -dependent MLC kinase (MLCK)<sup>33</sup>. It has been reported that traction forces alone can activate Piezo1 to generate local  $Ca^{2+}$  flickers in neural stem cells<sup>34</sup>. This process involves Light Chain Kinase regulated myosin-II<sup>34</sup>. Thus, Piezo1 mediates  $Ca^{2+}$  influx, that in turn can also promote Myosin-II contractile forces and maturation of FAs<sup>35</sup>. With Piezo1 inhibitors, there are nascent FAs since the lamellipodial actin extrusion and formation of nascent FAs does not involve a significant contraction force<sup>36</sup>.

In conclusion, Piezo1 channels function to translate mechanical cues that affect cell spreading. A change of local tension due to cell growth on the confined surface area triggers Piezo1 migration from the soma to the extrusion edges. Piezo1 has at least two roles at the cell edge. They open to create a  $Ca^{2+}$  influx, that activates  $Ca^{2+}$ -dependent contraction forces in the Rho-ROCK pathway, enabling FA formation and cell expansion. Inhibition of Piezo1 influx does not block the translocation of proteins, nor the growth of thin tail-like features showing that inhibition of ion influx is not the same as the knockout, so that Piezo may have other enzymatic activities.

## Materials and methods

**Substrate patterning.** Parallel fibronectin stripes 6  $\mu$ m wide with 10  $\mu$ m spacing were printed on a glass coverslip using standard microprinting techniques. Briefly, a PDMS stamp was fabricated using soft lithography. Coverslips were cleaned in a boiling mixture solution of ammonium hydroxide and hydrogen peroxide for 10 min, and were rinsed with ethanol and dried under UV light. The coverslips were then treated with plasma for 3 min to increase hydrophilicity. To print fibronectin on the coverslip, fibronectin (50  $\mu$ g/ml) was applied over the stamp and left for 1 h, and rinsed with PBS. The stamp was then pressed in contact with the coverslip. To reduce non-selective cell attachment, the patterned cover glass was immersed into a blocking reagent (0.2% Pluronic F-127) (Sigma-Aldrich) for 1 h. Finally, a ring-shaped thick PDMS wall was bound to the coverslip to form a dish containing a patterned glass bottom. The patterns were examined with NHS-Fluorescein dye (ThermoFisher Scientific) using a fluorescent microscope.

**Cell morphology evaluation.** The change in the morphology of the cells was quantified by its length to width aspect ratio calculated using ImageJ (NIH) and MATLAB. Brightfield images were imported in MATLAB and cells were identified from the background using “adaptive threshold” built-in the Image Segmenter app. At this stage, the output binary images included full cell length (cell body with tails, Fig. 1,c2). Next, an erosion was applied to the images which removed the fine structures in the image such as tails; this was followed by a dilation with the same parameter as the erosion to restore the cell body shapes while the tails were removed (cell body, Fig. 1,c3). The erosion and dilation set values remained the same for all the images to remove any bias and manual modification maintained minimal. Binary images were then transferred to ImageJ and major and minor axes of the best fitted ellipse were calculated using Fit Ellipse built-in function (Fig. 1,c4). The ratio of the major axis to the minor axis (L/W) of an ellipse was defined as the aspect ratio of a cell.

**Cell culture and Piezo1 cell lines.** Human embryonic kidney (HEK293T) cells (ATCC), and HEK cells stably expressing EGFP-tagged human Piezo1 (HEK293T-hP1)<sup>7</sup>, and Piezo1 knockout (P1KO) (kind gift from the Patapoutian group) were cultured in Dulbecco’s Modified Eagle Medium (DMEM) complemented with 10% fetal bovine serum (FBS) and 1% penicillin and streptomycin in culture flasks. The HEK-hP1 cell line was previously created by expressing a fluorescently tagged human Piezo1 called hPIEZO1-1591-EGFP5 into HEK293T<sup>25</sup>. The cDNA was integrated into the genome of cells using a lentivirus vector. The detail method is described previously<sup>25</sup>. For visualizing FAs, HEK-hP1 cells were co-transfected with 0.2 µg plasmid DNA of paxillin-mApple (generous gift from Michael Davidson) using transfection reagent Effectene (Qiagen, Valencia, CA), and were cultured for 24 h.

The cells in the flask were trypsinized and seeded onto the patterned substrates. Unattached cells were gently washed away using PBS after 10 min. During experiments, the chip was placed in a stage-top incubator (INUB-ZILCSD-F1-LU, Tokai Hit Co., Ltd, Japan) maintained at 37 °C and 5% CO<sub>2</sub>. Fluorescence imaging was done in DMEM without phenol red (Gibco, TX) to avoid background fluorescence. Isotonic saline solution was used for imaging GsMTx4 treated cells since DMEM reduces the potency of the peptide<sup>26</sup>.

**Immunostaining.** For staining, cells were fixed with 4% paraformaldehyde for 15 min. Permeabilization was done using 0.1% Triton X-100 (Sigma-Aldrich) for 15 min followed by blocking with 1% Bovine Serum Albumin (BSA, Sigma-Aldrich) for 1 h to avoid non-specific binding. Hoechst 33342 (1.6 µM, ThermoFisher) dye was then added to cells and incubated for 5 min at room temperature. Imaging was done in slow fade Gold Anti-fade Reagent (1:100, Invitrogen) in PBS to protect from photobleaching.

**Fluorescence imaging.** Images were acquired using an inverted microscope (Axiovert 200 M, Zeiss) with a CCD camera (AxioCam, Zeiss). Live cell images were obtained with two filter sets: (Ex: 470/40 nm; Em: 525/50 nm) and (Ex: 550/25, Em: 605/70), and a 63× oil immersion objective. The nucleus images were acquired with filter set (Ex: 365/40; Em: 445/50 nm). The B/W images were obtained using a 20× objective.

**Statistical analysis.** The aspect ratios were averaged over N cells from each panel and over a minimum of six experiments. Statistical data were shown as mean ± standard error of the means (s.e.m.). The data was analyzed using two-sample t-test for different cell types and paired sample t-test for the effect of drugs. P-values < 0.001 were considered to be statistically significant.

**Solution and chemicals.** GsMTx4 was purified and diluted in saline to a final concentration of 20 µM. Gadolinium chloride and Y27632 (all from Sigma-Aldrich, St. Louis, MO) were prepared to final concentrations of 60 µM and 30 µM, respectively.

Received: 10 December 2020; Accepted: 11 February 2021

Published online: 03 March 2021

## References

- Schwartz, M.A. Integrins and extracellular matrix in mechanotransduction. *Cold Spring Harb. Perspect. Biol.* **2** (2010).
- Katsumi, A., Orr, A. W., Tzima, E. & Schwartz, M. A. Integrins in mechanotransduction. *J. Biol. Chem.* **279**, 12001–12004 (2004).
- Ingber, D. E. Mechanosensation through integrins: cells act locally but think globally. *Proc. Natl. Acad. Sci. U S A* **100**, 1472–1474 (2003).
- Coste, B. *et al.* Piezo proteins are pore-forming subunits of mechanically activated channels. *Nature* **483**, 176–181 (2012).
- Coste, B. *et al.* Piezo1 and Piezo2 are essential components of distinct mechanically activated cation channels. *Science* **330**, 55–60 (2010).
- Lewis, A.H. & Grandl, J. Mechanical sensitivity of Piezo1 ion channels can be tuned by cellular membrane tension. *Elife* **4** (2015).
- Cox, C. D. *et al.* Removal of the mechanoprotective influence of the cytoskeleton reveals PIEZO1 is gated by bilayer tension. *Nat. Commun.* **7**, 10366 (2016).
- Syeda, R. *et al.* Piezo1 channels are inherently mechanosensitive. *Cell Rep.* **17**, 1739–1746 (2016).
- Li, J. *et al.* Piezo1 integration of vascular architecture with physiological force. *Nature* **515**, 279–282 (2014).
- Ranade, S. S. *et al.* Piezo1, a mechanically activated ion channel, is required for vascular development in mice. *Proc. Natl. Acad. Sci. U S A* **111**, 10347–10352 (2014).
- Jetta, D., Gottlieb, P.A., Verma, D., Sachs, F. & Hua, S.Z. Shear stress-induced nuclear shrinkage through activation of Piezo1 channels in epithelial cells. *J. Cell Sci.* **132** (2019).
- Gudipaty, S. A. *et al.* Mechanical stretch triggers rapid epithelial cell division through Piezo1. *Nature* **543**, 118–121 (2017).



13. Eisenhoffer, G. T. *et al.* Crowding induces live cell extrusion to maintain homeostatic cell numbers in epithelia. *Nature* **484**, 546–549 (2012).
14. He, L., Si, G., Huang, J., Samuel, A. D. T. & Perrimon, N. Mechanical regulation of stem-cell differentiation by the stretch-activated Piezo channel. *Nature* **555**, 103–106 (2018).
15. Cahalan, S.M. *et al.* Piezo1 links mechanical forces to red blood cell volume. *Elife* **4** (2015).
16. McHugh, B. J. *et al.* Integrin activation by Fam38A uses a novel mechanism of R-Ras targeting to the endoplasmic reticulum. *J. Cell Sci.* **123**, 51–61 (2010).
17. Pathak, M. M. *et al.* Stretch-activated ion channel Piezo1 directs lineage choice in human neural stem cells. *Proc. Natl. Acad. Sci. U S A* **111**, 16148–16153 (2014).
18. Koser, D. E. *et al.* Mechanosensing is critical for axon growth in the developing brain. *Nat. Neurosci.* **19**, 1592–1598 (2016).
19. Segel, M. *et al.* Niche stiffness underlies the ageing of central nervous system progenitor cells. *Nature* **573**, 130–134 (2019).
20. Suffoletto, K., Ye, N., Meng, F., Verma, D. & Hua, S. Z. Intracellular forces during guided cell growth on micropatterns using FRET measurement. *J. Biomech.* **48**, 627–635 (2014).
21. Thery, M. *et al.* The extracellular matrix guides the orientation of the cell division axis. *Nat. Cell Biol.* **7**, 947–953 (2005).
22. Vedula, S. R. *et al.* Emerging modes of collective cell migration induced by geometrical constraints. *Proc. Natl. Acad. Sci. U S A* **109**, 12974–12979 (2012).
23. Suffoletto, K., Jetta, D. & Hua, S. Z. E-cadherin mediated lateral interactions between neighbor cells necessary for collective migration. *J. Biomech.* **71**, 159–166 (2018).
24. Hung, W. C. *et al.* Confinement sensing and signal optimization via Piezo1/PKA and myosin II pathways. *Cell Rep.* **15**, 1430–1441 (2016).
25. Maneshi, M. M., Ziegler, L., Sachs, F., Hua, S. Z. & Gottlieb, P. A. Enantiomeric Abeta peptides inhibit the fluid shear stress response of PIEZO1. *Sci. Rep.* **8**, 14267 (2018).
26. Bae, C., Sachs, F. & Gottlieb, P. A. The mechanosensitive ion channel Piezo1 is inhibited by the peptide GsMTx4. *Biochemistry* **50**, 6295–6300 (2011).
27. Yao, M. *et al.* Force-dependent Piezo1 recruitment to focal adhesions regulates adhesion maturation and turnover specifically in non-transformed cells. *BioRxiv* (2020).
28. Maneshi, M. M., Gottlieb, P. A. & Hua, S. Z. A microfluidic approach for studying piezo channels. *Curr. Top. Membr.* **79**, 309–334 (2017).
29. Douguet, D. & Honore, E. Mammalian mechanoelectrical transduction: Structure and function of force-gated ion channels. *Cell* **179**, 340–354 (2019).
30. Murthy, S.E. *et al.* OSCA/TMEM63 are an evolutionarily conserved family of mechanically activated ion channels. *Elife* **7** (2018).
31. Servin-Vences, M.R., Moroni, M., Lewin, G.R. & Poole, K. Direct measurement of TRPV4 and PIEZO1 activity reveals multiple mechanotransduction pathways in chondrocytes. *Elife* **6** (2017).
32. Gnanasambandam, R. *et al.* GsMTx4: Mechanism of inhibiting mechanosensitive ion channels. *Biophys. J.* **112**, 31–45 (2017).
33. Eddy, R. J., Pierini, L. M., Matsumura, F. & Maxfield, F. R. Ca<sup>2+</sup>-dependent myosin II activation is required for uropod retraction during neutrophil migration. *J. Cell Sci.* **113**(Pt 7), 1287–1298 (2000).
34. Ellefsen, K. L. *et al.* Myosin-II mediated traction forces evoke localized Piezo1-dependent Ca(2+) flickers. *Commun. Biol.* **2**, 298 (2019).
35. Ye, N. *et al.* Direct observation of alpha-actinin tension and recruitment at focal adhesions during contact growth. *Exp. Cell Res.* **327**, 57–67 (2014).
36. Giannone, G. *et al.* Lamellipodial actin mechanically links myosin activity with adhesion-site formation. *Cell* **128**, 561–575 (2007).

## Acknowledgements

This work was supported by National Science Foundation (CMMI-2015964 and CMMI-1537239). We thank Dr. Philip Gottlieb at University at Buffalo for helpful discussions.

## Author contributions

D.J. and M.R.B.F. designed and performed the experiments and analyzed data; F.S. interpreted data and edited manuscript; K.M. analyzed data; S.Z.H. designed the experiments, analyzed and interpreted data, and wrote the manuscript.

## Competing interests

The authors declare no competing interests.

## Additional information

**Supplementary Information** The online version contains supplementary material available at <https://doi.org/10.1038/s41598-021-84427-y>.

**Correspondence** and requests for materials should be addressed to S.Z.H.

**Reprints and permissions information** is available at [www.nature.com/reprints](http://www.nature.com/reprints).

**Publisher's note** Springer Nature remains neutral with regard to jurisdictional claims in published maps and institutional affiliations.



**Open Access** This article is licensed under a Creative Commons Attribution 4.0 International License, which permits use, sharing, adaptation, distribution and reproduction in any medium or format, as long as you give appropriate credit to the original author(s) and the source, provide a link to the Creative Commons licence, and indicate if changes were made. The images or other third party material in this article are included in the article's Creative Commons licence, unless indicated otherwise in a credit line to the material. If material is not included in the article's Creative Commons licence and your intended use is not permitted by statutory regulation or exceeds the permitted use, you will need to obtain permission directly from the copyright holder. To view a copy of this licence, visit <http://creativecommons.org/licenses/by/4.0/>.

© The Author(s) 2021